HEFAT2014
10th International Conference on Heat Transfer, Fluid Mechanics and Thermodynamics
14 – 16 July 2014
Orlando, Florida

NEW METHOD FOR THE IDENTIFICATION OF TWO-PHASE FLOW PATTERNS IN A MINICHANNEL

G. Górski, R. Mosdorf*.
*Author for correspondence
Department of Mechanics and Applied Computer Science, Faculty of Mechanical Engineering,
Bialystok University of Technology,
Wiejska 45 C, 15-351 Bialystok,
Poland,
E-mail: r.mosdorf@pb.edu.pl

ABSTRACT

In the paper the new method for the identification of two-phase flow patterns in a minichannel has been proposed. The two-phase flow (water-air) occurring in rectangular minichannel (3x3 mm) has been analysed. It was tested whether the change of the two-phase flow pattern was accompanied by changing the dynamics of two-phase flow. The signal from laser - phototransistor sensor, recorded during the experiment, was analysed. The proposed method was based on the recurrence plot and the principal component analysis.

The thirteen coefficients describing the dynamics of considered data (results of recurrence quantification analysis) have been treated as a set of variables describing the dynamics of two phase flow patterns. The principal component analysis (PCA) has been used to obtain the set of independent variables, which characterise the dynamics of system under consideration. Obtained results show that the first two components explain the 91% of input data variation. It has been shown that in the plots of two first components the points are grouped in the four separated clusters, which correspond to different flow patterns (two types of bubbly flow, and two types of slug flow - small and long slugs).

INTRODUCTION

Numerous experimental studies carried out in recent years in many universities indicate that the two-phase flows in minichannels are accompanied by fluid behaviours different from those observed in traditional channels [1, 2]. Despite many experimental and theoretical researches in the literature there is no clear classification of patterns of two-phase flow and types of channels [3].

The identification of flow patterns in minichannels often depends on the subjective evaluation of the observer and used experimental technique. For parameters characterizing the transition between flow patterns the two phase flow is usually unsteady. In such situation the criteria based on average values of the various parameters are not suitable for identification the border between flow patterns. Therefore, the new criterion based on properties of dynamics of two phase flow is needed.

NOMENCLATURE

I		Mutual information
n, N		Number of samples
p		Probability
q	[l/min]	Volume flow rate
R		Recurrence plot
RR		Recurrence rate
t		Time
x	[V]	Signal from laser-phototransistor sensor

Special characters

τ	Time delay
ε	Recurrence plot parameter
Θ	Heaviside function

Subscripts

a	Air
w	Water

Wang at. al in the paper [9] shown that the non-linear analysis, which allows us the identification of flow patterns of the mixture of oil-gas-water. The results of non-linear analysis of temperature and pressure fluctuations in microchannels are discussed by Mosdorf at.al in the paper [10]. Wang at. al in the paper [11], used the non-linear analysis of the pressure fluctuations to identify the flow structures of air in water. Methods characterizing the non-linear dynamics of the flow of oil-water [12] were useful for identification of the flow patterns and for assessment of the complexity of these patterns. Jin at al. in the paper [13] shows that the correlation dimension and Kolmogorov entropy are sufficient to identify the flow patterns. Faszczewski at al. in the paper [14] used the recurrence plot method to analyse the flow patterns in a vertical mini channel.

It has been shown that this method allows us to determine the parameters which define the borders between flow patterns.

The subject of the research is the development of methods for identifying the types of flow patterns which occur during the movement of the liquid-gas mixture in the minichannel. It was assumed that the loss of stability of the two-phase flow pattern and the formation of the new flow pattern is accompanied by the change of parameters describing the dynamics of two-phase flow. The determination of those parameters requires an analysis of the dynamics of two-phase flow. The method proposed in the paper is based on the recurrence plot and the principal component analysis. The signal from laser - phototransistor sensor was analysed.

EXPERIMENTAL SETUP, MEASUREMENT TECHNIQUES

During the experiment it was analysed the data recorded for different flow patterns (water-air at 21^{o} C) in a rectangle channel 3x3 mm. In Figure 1 the schema of experimental stand is presented. Due to the size of the minichannel the obtaining the bubbly flow inside it requires the usage of a special generator of mini bubbles (8 - Figure 1a). The proportional pressure regulator (Metal Work Regtronic with an accuracy of 1 kPa) was used to maintain the constant overpressure in the supply tank (10 - Figure 1a) - the overpressure was 50 kPa. Flow patterns were recorded with using the Casio EX-F1 digital camera at 1200 fps (336 x 96 pixels). Pressure difference between the inlet and outlet of minichannel was measured using the silicon pressure sensor MPX12DP (range 0 - 10 kPa, sensitivity 5.5 mV/kPa, response time 1 ms, accuracy ±0.05 kPa). The amount of vapour flowing through the minichannel was measured by laser-phototransistor sensor (3 - Figure 1a). Data from the sensors was acquired by the acquisition system (Data translation 9804, an accuracy of 1 mV for voltages in the range of -10 V to 10 V), (11 - Figure 1a) at a sampling rate of 1 kHz.

The content of the minichannel (bubbles or liquid) has been qualitatively assessed using the laser - phototransistor sensor (3 - Figure 1a). The schema of laser-phototransistor sensor is presented in Figure 1b. The sensor consisted with a laser which generated the laser beam with a diameter of 3 mm, the lens and silicon sensor placed in focal point of lens. Bubbles inside the minichannel bend the light which modifies the light intensity on the silicon sensor. When the channel is filled with water, the sensor generates a high voltage signal. When the bubble or slug occurs inside the minichannel, then the sensor generates a low voltage signal (about the 3 V). However, when the front of slug or bubble is passing through the laser beam, then the sensor voltage level drops to about 2 V. Small voltage drops below the maximum voltage level indicate that small bubbles are in the minichannel. The above properties of laser - phototransistor sensors allow us to use the signal from sensors for qualitative assessment of the presence of bubbles or slugs in the minichannel.

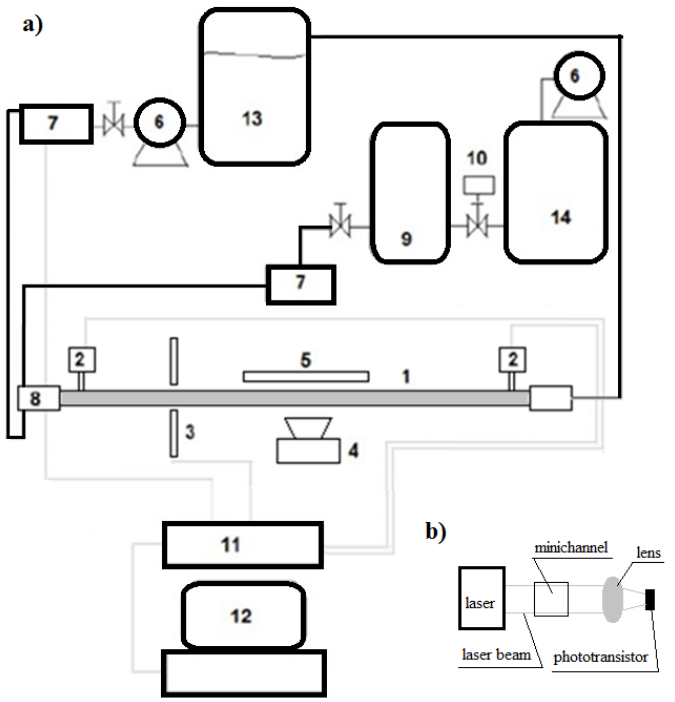

Figure 1 Scheme of experimental stand. a) Experimental setup: 1. minichannel, 2. pressure sensors (MPX12DP), 3. laser-phototransistor sensor. 4. Casio EX-FX1 camera, 5. lighting, 6. pumps (air or water), 7. flow meters. 8. mini bubbles generator, 9. air tank, 10. automatic valve to maintain a constant pressure in the tank 9, 11. data acquisition station (DT9800), 12. computer, 13. water tank, 14 air tank. b) Schema of laser-phototransistor sensor.

In Figure 2 it has been shown the examples of signal recorded from the laser-phototransistor sensor for different air volume flow rates and almost constant liquid flow rate. In each charts the examples of flow pattern occurring in the minichannel have been presented.

In the present paper, the three groups of time series have been considered. The two groups of time series were recorded in the same conditions but for different time periods. The third group of time series was recorded for higher water flow rate $q_w = 0.17$ l/min.

NON-LINEAR DATA ANALYSIS

Attractor reconstruction

The analysis of attractor of non-linear dynamical system gives us information about the properties of the system such as system complexity and its stability. In non-linear analysis the reconstruction of attractor in a certain embedding dimension is carried out using the stroboscope coordination [17]. In this method the subsequent co-ordinates of attractor points are calculated basing on the subsequent samples, between which the distance is equal to time delay τ. The time delay is a multiplication of time between the samples. The subsequent co-ordinates of attractor points are as follows [17].

$$\{x(t), x(t+\tau), ..., x[t+(n-1)\cdot\tau]\} \quad (1)$$

where x is a measure quantity.

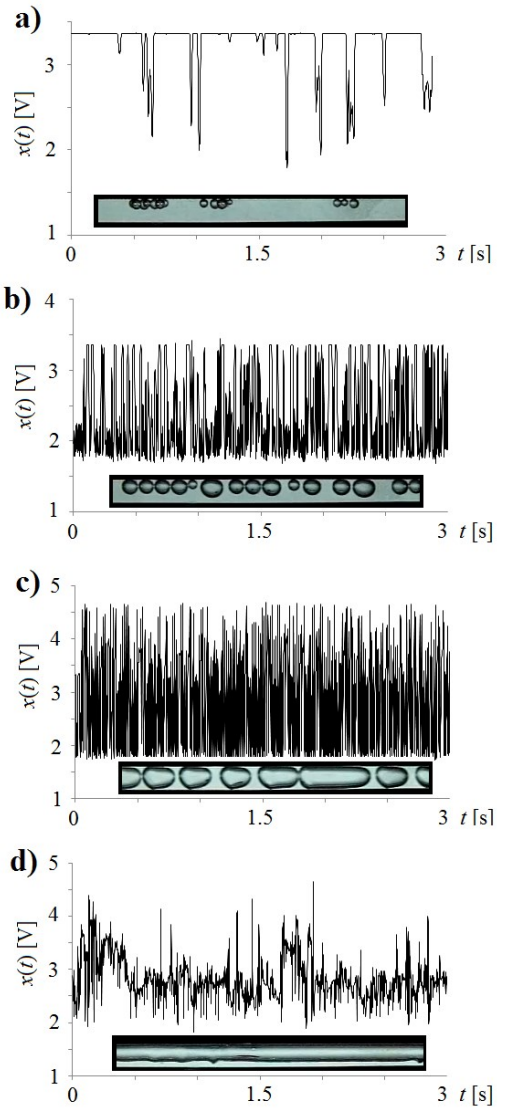

Figure 2 Example of time series from laser-phototransistor sensor recorded during the experiment. a) q_w = 0.056 l/min, q_a = 0.001 l/min, b) q_w = 0.058 l/min, q_a = 0.0424 l/min, c) q_w = 0.059 l/min, q_a = 0.1 l/min d) q_w = 0.056 l/min, q_a = 0.4 l/min.

In Figure 3 it has been shown the 3D attractor reconstruction from signals recorded from the laser-phototransistor sensor.

The image of the attractor in n-dimensional space depends on the time delay - τ. When the time delay is too small, the attractor gets flattened, that makes further analysis of its structure impossible [17,18]. The mutual information between time series: $x(t)$ and $x(t+\tau)$ can be used to determine the proper time delay for reconstruction of attractors.

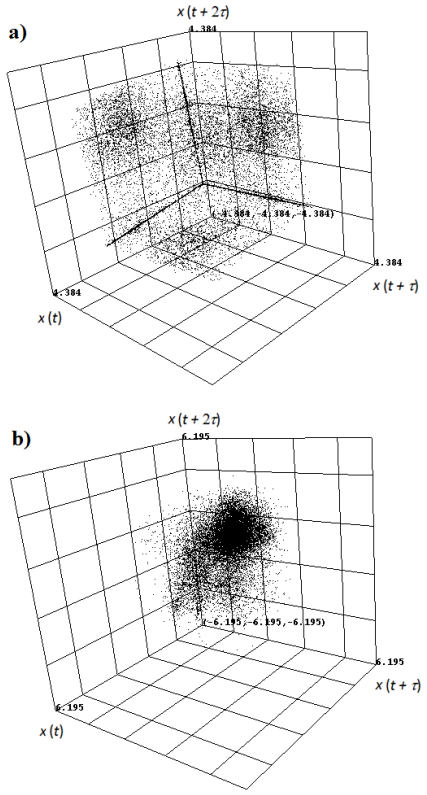

Figure 3 The attractor reconstruction for time series of laser-phototransistor signal for τ = 70. a) q_w = 0.059 l/min, q_a = 0.0127 l/min. b) q_w = 0.057 l/min, q_a = 0.4 l/min.

As τ is increased, the mutual information decreases and then usually rises again [5,6,16]. The time delay for which the mutual information obtains the first minimum is a proper value of τ. The mutual information of $x(t)$ and $x(t+\tau)$ can be defined as [5,6]:

$$I(x(t), x(t+\tau)) = \sum_{x(t+\tau)} \sum_{x(t)} p[x(t), x(t+\tau)] log_2 \left\{ \frac{p[x(t), x(t+\tau)]}{p[x(t)]p[x(t+\tau)]} \right\} \quad (2)$$

where $p[x(t),x(t+\tau)]$ is the joint probability distribution function of $x(t)$ and $x(t+\tau)$, and $p[x(t)]$ and $p[x(t+\tau)]$ are the marginal probability distribution functions of x and $x(t+\tau)$.

The mutual information is equal to zero if $x(t)$ and $x(t+\tau)$ are independent random variables.

In Figure 4 it has been shown the mutual information functions vs time delay (number of samples) for the time series recorded from the laser-phototransistor sensor for q_w = 0.059 l/min, q_a = 0.0127 l/min. The function reaches its first minimum at $\tau \sim 70$ samples.

The false nearest neighbour algorithm [16] has been used for estimation of the proper embedding dimension of attractors. In this method the changes of number of neighbouring points in embedding space with increasing embedding dimension is examined. For each point x_i the distances to its nearest neighbour x_j are calculated, in m and in m+1 dimensional space. The point is treated as a false neighbour when the distance

between points (i, j) becomes large in case when the embedding space dimension increases.

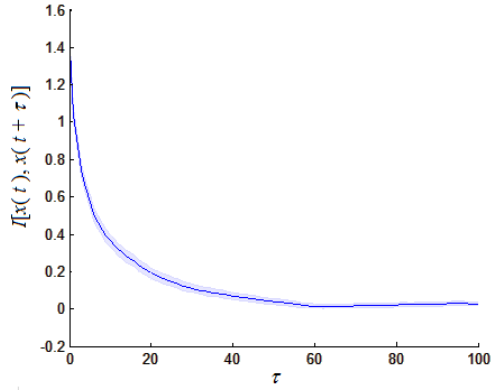

Figure 4 The mutual information functions vs time delay (number of samples) for the time series recorded from the laser-phototransistor sensor for q_w = 0.059 l/min, q_a = 0.0127 l/min. The calculations have been made using the Matlab Toolbox [16].

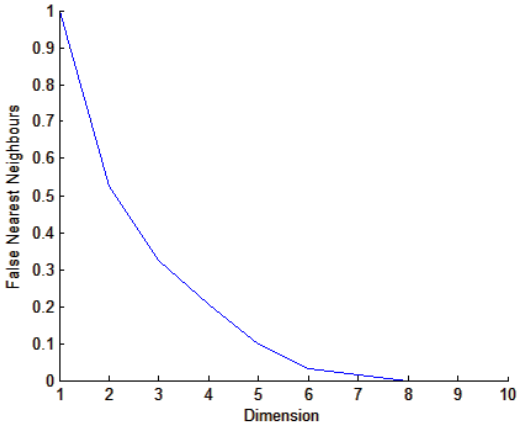

Figure 5 The changes of number of false nearest neighbours points [4] for the time series recorded from the laser-phototransistor sensor for q_w = 0.059 l/min, q_a = 0.0127 l/min. The calculations have been made using the Matlab Toolbox [16].

The number of false neighbours is calculated for the whole time series and for several dimensions until the fraction of false points reaches zero. Such dimension is treated as a proper embedding dimension for attractor reconstruction. In Figure 5 it has been shown the changes of percent of number of false neighbours vs the embedding dimension. In case under consideration the proper embedding dimension for attractor reconstruction is equal to 8.

Recurrence plot

Recurrence plot is a technique of visualization of the recurrence of states x_i in m-dimensional phase space. The recurrence of states at time i and at a different time j is marked with black dots in the 2D plot, where both axes are time axes. The recurrence plot is defined as [15]:

$$R_{i,j} = \Theta\left(\varepsilon - \left\|x_i - x_j\right\|\right),\ x_i \in \Re^m,\ i,j - 1 \ldots N \tag{3}$$

where N is the number of considered states x_i, ε is a threshold distance, $\|\cdot\|$ is a norm and $\Theta(\cdot)$ is the Heaviside function.

A line parallel to main diagonal line occurs when a segment of the trajectory runs parallel to an another segment and the distance between trajectories is less than ε. The length of this diagonal line is determined by the duration of this phenomenon. A vertical (horizontal) line indicates a time in which a state does not change or changes very slowly. The diagonal lines (structures) periodically occurred in the recurrence plot are characteristic for periodic system [15]. In Figure 6 it has been shown the recurrence plots of signal from laser – phototransistor sensor for different flow patterns in minichannel.

Recurrence rate, RR, is a measure of the percentage of recurrence points in the recurrence plot. It is defined as follows [15]:

$$RR = \frac{1}{N^2}\sum_{i,j=0}^{N} R_{i,j} \tag{4}$$

The value of RR corresponds to the correlation sum.

The number of points which appears in the recurrence plot depends on the value of ε. Recurrence rate is a non-linear function of ε. In Figure 7 it is presented the function $RR(\varepsilon)$ obtained for time series under consideration. Strong nonlinearity of function $RR(\varepsilon)$ is visible for the small value of ε. For higher value of ε the nonlinearity becomes smaller (the function becomes quasi linear). It has been assumed that the lowest value of ε in the linear part of function $RR(\varepsilon)$ is a proper value of ε for the reconstruction of recurrence plot. For time series under consideration it is equal to 3 (Figure 7).

The quantitative recurrence analysis generates the coefficients which describe the dynamics of two-phase flow patterns. The thirteen coefficients [15, 16] have been considered as a set of variables describing the dynamics of two phase flow patterns. The calculations have been made using the Matlab Toolbox [16].

The following properties of the recurrence plot have been considered [16]:

1. The overall quantity characteristic of the recurrence plot is described by the **recurrence rate**, RR eq(4).
2. The characteristics of diagonal lines are described by:
   Determinism:

$$DET = \frac{\sum_{l=lmin}^{N} lP^{\varepsilon}(l)}{\sum_{i,j}^{N} R_{i,j}^{m,\varepsilon}} \tag{5}$$

   (where $P(l)$ is the distribution of the lengths of diagonal structures and N is the absolute number of diagonal lines);

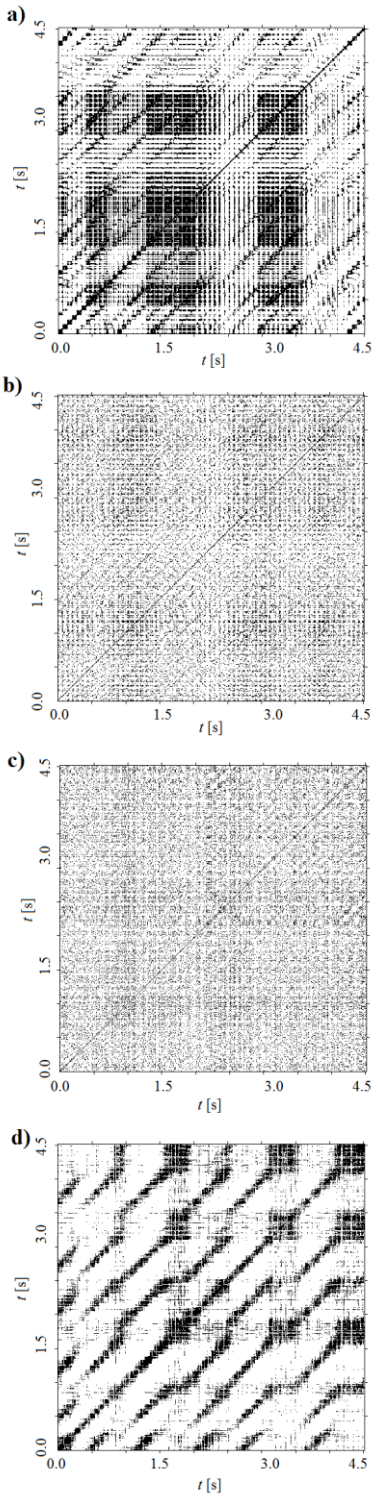

Figure 6 Recurrence plots for embedding dimension 8, time delay 70 and $\varepsilon = 3$. a) $q_w = 0.056$ l/min, $q_a = 0.001$ l/min, b) $q_w = 0.058$ l/min, $q_a = 0.0424$ l/min, c) $q_w = 0.059$ l/min, $q_a = 0.1$ l/min d) $q_w = 0.056$ l/min, $q_a = 0.4$ l/min. The calculations have been made using the Matlab Toolbox [16].

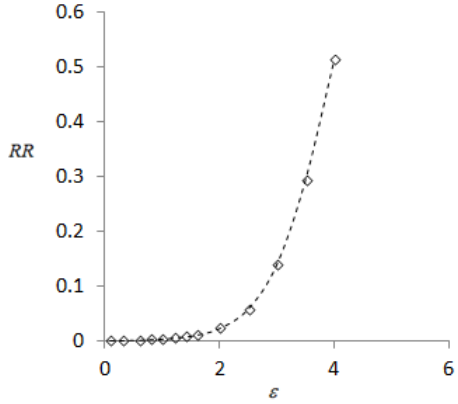

Figure 7 Recurrence rate, *RR*, vs ε for the time series recorded from the laser-phototransistor sensor for $q_w = 0.059$ l/min, $q_a = 0.0127$ l/min. The calculations have been made using the Matlab Toolbox [16].

Averaged length of the diagonal line:

$$AVG = \frac{\sum_{l=l_{\min}}^{N} lP(l)}{\sum_{l=l_{\min}}^{N} P(l)} \tag{6}$$

where $p(l) = \frac{P^{\varepsilon}(l)}{\sum_{l=lmin}^{N} P^{\varepsilon}(l)}$;

Length of the longest diagonal line;
Entropy of occurrence of the diagonal line lengths:

$$ENTR = -\sum_{l=lmin}^{N} p(l) ln\, p(l); \tag{7}$$

3. The characteristics of vertical lines are described by:

Laminarity:
The percentage of recurrent points which belong to the vertical structures (lines)

$$LAM = \frac{\sum_{v=vmin}^{N} vP^{\varepsilon}(v)}{\sum_{v=1}^{N} vP^{\varepsilon}(v)}; \tag{8}$$

where $P(v)$ denotes the distribution of the lengths of vertical structures;

Trapping time:
The average length of vertical line structures:

$$TT = \frac{\sum_{v=vmin}^{N} vP^{\varepsilon}(v)}{\sum_{v=vmin}^{N} P^{\varepsilon}(v)}; \tag{9}$$

Length of the longest vertical line;
Recurrence time of 1st type, the recurrence time of 2nd type:

The recurrence time is calculated as the distance between the points belonging to the vertical lines in RP. In case of recurrence time of the first type T^1, all points of RP are considered. Such value of T^1 depends on the trajectory density and value of ε.

In case of recurrence time of the second type T^2, the vertical distances between the pairs "white"

pixel/"black" pixel in the columns are measured. The T^2 accurately estimates the period of time series. This type of recurrence time is related to the entropy and to the information dimension of the attractor [20, 21].

Recurrence period density entropy:

Little et al. [22] developed a Recurrence Period Density Entropy method. In this method the recurrences into the neighborhood, ε, of each points are tracked, and such obtained time intervals are used for construction of the histogram of recurrence times. This histogram is used for calculation of the recurrence period density function. The normalized entropy of this density has a form [22].

$$H_{norm} = -(lnT_{max})^{-1} \sum_{t=1}^{T_{max}} p(t) lnp(t) \quad (10)$$

The value of H_{norm} changes in the range from zero to one. For the periodic signals, $H_{norm} = 0$ whereas for the uniform white noise, $H_{norm} = 1$.

4. Overall characteristic of recurrence plot (based on the analysis of complex network) is described by clustering and transitivity coefficients. In this approach the recurrence plot is treated as the adjacency matrix of a complex network [23].

Clustering coefficient:

The clustering coefficient is a probability that two neighbours (i.e. recurrences) of any state are also neighbours [25]. It is obtained as the average of the local clustering coefficient. The clustering coefficient is calculated as follows:

$$C = \sum_{i=1}^{N} \frac{\sum_{j,k=1}^{N} R_{i,j}^{m,\varepsilon} R_{j,k}^{m,\varepsilon} R_{k,i}^{m,\varepsilon}}{\sum_{j=1}^{N} R_{i,j}^{m,\varepsilon}} \quad (11)$$

Transitivity:

The clustering coefficient places more weight on the low degree nodes, while the transitivity ratio places more weight on the high degree nodes. The transitivity coefficient is calculated as follows:

$$C_T = \sum_{i=1}^{N} \frac{\sum_{i,j,k=1}^{N} R_{i,j}^{m,\varepsilon} R_{j,k}^{m,\varepsilon} R_{k,i}^{m,\varepsilon}}{\sum_{i,j,k=1}^{N} R_{i,j}^{m,\varepsilon} R_{k,i}^{m,\varepsilon}} \quad (12)$$

IDENTIFICATION OF TWO-PHASE FLOW PATTERNS

The coefficients generated by the quantitative recurrence analysis describe the different aspects of dynamical system but they are correlated. Therefore, they cannot be treated as independent variables describing the system dynamics. For that reason, the principal component analysis (PCA) has been used to obtain the set of independent variables which characterise the dynamics of the system under consideration.

The principal component analysis is a method that uses the orthogonal transformation to convert an input set of data into a new set of data, in a new set of coordinates called the principal components. This transformation is defined in such a way that the data has the largest possible variance around the first principal component. For the successive components the variance of data decreases.

In PCA method the matrix, A, containing the values of 13 coefficients characterising the RP-s (name of columns) and rows representing the number of measurement (in case under consideration it was 13 measurements) is analysed. In the first step of analysis the data in columns of matrix A is normalised. In the next step the covariance matrix is created.

$$C = (AA^T)/(n-1) \quad (13)$$

where n is a number of measurements.

The dimension of covariance matrix is 13x13. Then, the eigenvectors and eigenvalues of the covariance matrix are calculated using the SVD decomposition.

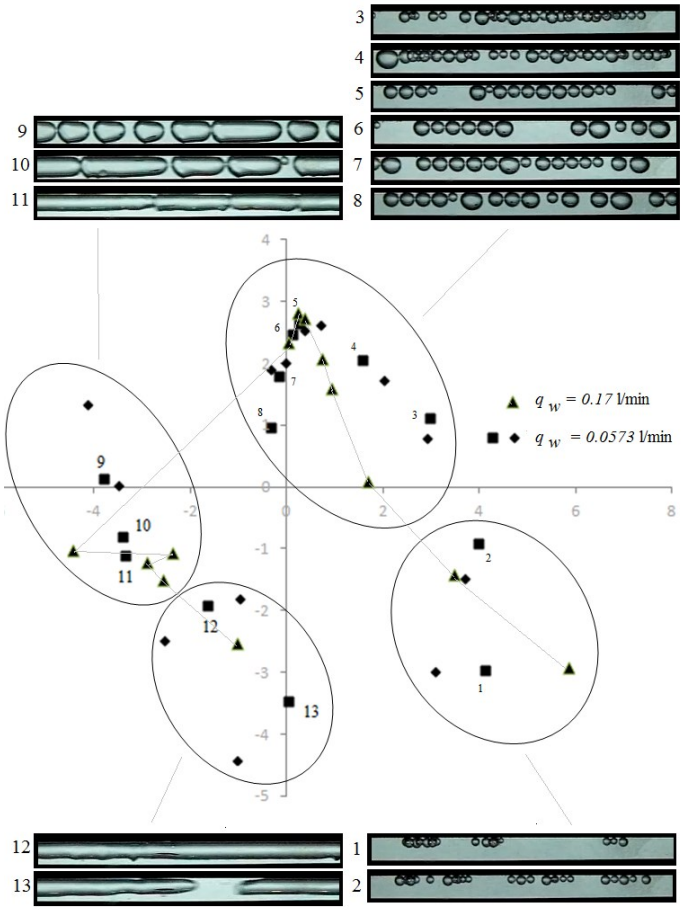

Figure 8 2D map of different patterns of two phase flow in minichannel in the space of two first components.

In this method a rectangular matrix A can be broken down into the product of three matrices - an orthogonal matrix U, a diagonal matrix S and the transpose of an orthogonal matrix V. The SVD decomposition has the following form:

$$A_{mn} = U_{mm} S_{mn} V^T_{nn} \quad (14)$$

where S is a diagonal matrix containing the square roots of ordered eigenvalues. The columns of U are orthonormal eigenvectors of AA^T, the columns of V are orthonormal eigenvectors of A^TA.

Columns of matrix U contain the eigenvectors of the covariance matrix which define the new coordinates characterising the data. In the end step of analysis the data is expressed in the new coordinates (called components) by the multiplication of eigenvectors by data matrix.

The results of calculations show that the two first components explain the $48\% + 43\% = 91\%$ of input data variation. In Figure 8 it has been shown the plot of data in the space of the two first components. The points are gathered in the four separated groups, which correspond to different flow patterns. In Figure 8 there is presented the results of analysis of three groups of time series under consideration.

CONCLUSION

In the paper the new method of two-phase flow identification has been presented. The method is based on the analysis of dynamics of signal recorded from the laser-phototransistor sensor. It has been shown that in the plots of two first components the points are grouped in the four separated areas, which correspond to different flow patterns (two types of bubbly flow and two types of slug flow - small and long slugs).

In the proposed method, the quantitative recurrence analysis uses the normalized signals, so the average values of the signal do not affect the results of the analysis. Despite of the neglect of quantitative signal characteristics, the qualitative analysis of its dynamics allows us for the identification of the two-phase flow patterns. This confirms that this type of analysis can be used to identify the two-phase flow patterns in the minichannel. The final verification of the proposed method requires a much larger number of analyses of different types of two-phase flows.

Acknowledgement

The project was funded by the National Science Centre, Poland - the number of decision: DEC-2013/09/B/ST8/02850

REFERENCES

[1] Zhao L., Rezkallah K.S., (1993) Gas–liquid flow patterns at microgravity condition, International Journal Multiphase Flow 19, 751-763.

[2] Wongwises S., Pipathattakul M. (2006) Flow pattern, pressure drop and void fraction of two-phase gas–liquid flow in an inclined narrow annular channel. Experimental Thermal and Fluid Science, 30, 345-354.

[3] Chen L., Tian Y.S. and Karayiannis T.G., (2006) The effect of tube diameter on vertical two-phase flow regimes in small tubes. International Journal of Heat and Mass Transfer 49, 4220-4230.

[4] M. B. Kennel, R. Brown, and H. D. I. Abarbanel, Determining embedding dimension for phase-space reconstruction using a geometrical construction, Phys. Rev. A **45**, (1992), 3403.

[5] A.M. Fraser, H.L. Swinney, Independent coordinates for strange attractors from mutual information, Phys. Rev. A 33 (1986) 1134–1140.

[6] W. Liebert, H. G. Schuster, Proper choice of time delay for the analysis of chaotic time series. Phys. Lett., A 142 (1989) 107.

[7] T. Parker, L. Chua, Practical numerical algorithms for chaotic systems, Springer, New York, 2000

[8] Kandlikav S.G. (2002) Fundamental issues related to flow boiling in minichannels and microchannels, Experimental Thermal and Fluid Science, 26, 389-407.

[9] Wang Z.Y., N.D.Jin, Z.K.Gao, Y.B.Zong, T.Wang. (2010a). Nonlinear dynamical analysis of large diameter vertical upward oil–gas–water three-phase flow pattern characteristics. Chemical Engineering Science 65, 5226–5236.

[10] Mosdorf R., Cheng P., Wu H.Y., Shoji M., (2005), Non-linear analyses of flow boiling in microchannels. Internationa Journal of Heat and Mass Transfer 48, 4667–4683.

[11] Wang S.F., R. Mosdorf, M. Shoji. (2003) Nonlinear analysis on fluctuation feature of two-phase flow through a T-junction. International Journal of Heat and Mass Transfer 46, 1519–1528.

[12] Yan-Bo Zong, Ning-De Jin, Zhen-Ya Wang, Zhong-Ke Gao, Chun Wang. (2010) Nonlinear dynamic analysis of large diameter inclined oil–water two phase flow pattern. International Journal of Multiphase Flow 36, 166–183

[13] Jin N.D., X.B. Nie, Y.Y. Ren, X.B. Liu. (2003) Characterization of oil/water two-phase flow patterns based on nonlinear time series analysis. Flow Measurement and Instrumentation 14, 169-175.

[14] Faszczewski M., G. Górski, R. Mosdorf, (2012), Applying Recurrence Plots to Identify Borders Between Two-Phase Flow Patterns in Vertical Circular Mini Channel. Acta Mechanica et Automatica, 6, 31-36.

[15] N. Marwan, M. C. Romano, M. Thiel, J. Kurths, (2007) Recurrence Plots for the Analysis of Complex Systems, Physics Reports, 438(5-6), 237-329.

[16] Norbert Marwan, Cross Recurrence Plot Toolbox for Matlab, Ver. 5.15, Release 28.10, http://tocsy.pik-potsdam.de

[17] Schuster H.G. (1993) Chaos deterministyczny – wprowadzenie, Wydawnictwo Naukowe PWN, Warszawa.

[18] Awrejcewicz, J., Mosdorf, R. (2003). Analiza numeryczna wybranych zagadnien dynamiki chaotycznej, Wydawnictwo Naukowo-Techniczne, Warsaw, (in Polish).

[19] Baker G.L., Gollub J.P. (1998) Wstęp do dynamiki układów chaotycznych, Wydawnictwo Naukowe PWN, Warszawa.

[20] Jianbo Gao, Yinhe Cao, Jing Hu. (2005) Recurrence Time Distribution, Renyi Entropy, and Pattern Discovery. Conference on Information Sciences and Systems, The Johns Hopkins University, March 16–18, 2005, http://www.gao.ece.ufl.edu/my_paper/rec-ciss2005.pdf.

[21] Jianbo Gao, Jing Hu. (2013) Fast monitoring of epileptic seizures using recurrence time statistics of electroencephalography. Front Comput Neurosci. 7: 122. Published online 2013 October 1. doi: 10.3389/fncom.2013.00122.

[22] M.A. Little, P.E. McSharry, S.J. Roberts, D.A.E. Costello, I.M. Moroz, (2007), Exploiting nonlinear recurrence and fractal scaling properties for voice disorder detection, BioMedical Engineering OnLine6 (23).

[23] Norbert Marwana, Jonathan F. Dongesa, Yong Zoua, Reik V. Donnera, Jürgen Kurthsa, (2009), Complex network approach for recurrence analysis of time series. Physics Letters A, Volume 373, Issue 46, Pages 4246–4254